Aerodynamic Design Features of the DC-9

RICHARD S. SHEVELL* AND ROGER D. SCHAUFELE†
Douglas Aircraft Company Inc., Long Beach, Calif.

The DC-9 aerodynamic design features discussed include the aft-engine T-tail arrangement, wing planform, airfoils, high-lift systems, nacelle-pylon design, and aerodynamic control systems. The aft-engine design is shown to have distinct advantages for the DC-9. There are two DC-9's: the Series 10, without leading-edge devices and therefore with airfoils having exceptional maximum lift capability; and the Series 30, with a longer fuselage, leading-edge devices, and airfoils more oriented toward minimum high-speed drag. The discussion concentrates on design areas associated with the aft-engine T-tail configuration such as the solution of the deep-stall problem and the design of the nacelle-pylon-fuselage area to minimize high Mach number drag. Causes of "locked-in" deep stall are shown to be related to the combined effects of wing and nacelle wakes and fuselage vortices on the horizontal tail. The DC-9 configuration has enough nose-down pitching moment capability to eliminate the possibility of locked-in deep stall. An analog simulator was used successfully to interpret extensive deep-stall wind-tunnel data. Flight-test results in all flight regimes verified the predictions of analytical methods and wind-tunnel tests.

1. Introduction

THE Douglas DC-9 series is intended to satisfy the need for a highly reliable, economical, short-range, high-performance jet transport. The purpose of this paper is to review the more significant aerodynamic design features of the DC-9 Series 10, the first of the series, and outline the aerodynamic development program. Later developments in the DC-9 series will be described briefly.

The pertinent physical characteristics of the DC-9 Series 10 are shown in Fig. 1. The DC-9 Series 10 has a wing area (934 ft²) less than that of a DC-3, a payload capacity exceeding that of a DC-7, and very nearly the cruise speed of a DC-8. Figure 2 summarizes the payload-range and takeoff performance of the DC-9 Series 10.

2. Major Aerodynamic Design Decisions

The first step in the evolution of an airplane design is the definition of general size and layout. Since the desired size of the DC-9 and the available engine types dictated a two-engine design, the first major configuration decision was that of wing configuration.

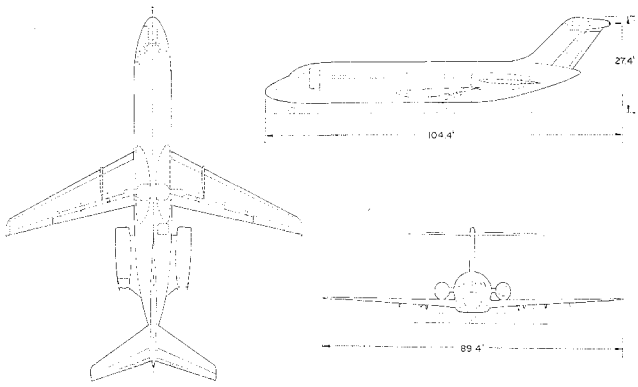

Fig. 1 General arrangement of DC-9 Series 10.

Presented as Preprint, 65-738 the AIAA/RAeS/JSASS Aircraft Design and Technology Meeting, Los Angeles, Calif., November 15–18, 1965; submitted December 9, 1965; revision received July 14, 1966.

* Chief, Aerodynamics Section. Member AIAA.
† Assistant Chief, Aerodynamics Section. Member AIAA.

Wing Configuration

The cruise speed was to be as high as was economically consistent with the short-field-length performance required for the DC-9. A high-speed cruise Mach number of 0.80 was selected, and various combinations of wing sweep angles and wing thicknesses were studied. The optimum combination is defined as the one that yields the lowest operating cost for a given cruise speed, payload-range ability, and field-length requirement. The results of our studies showed that 24° of sweep at the quarter-chord line was approximately the optimum. The wing thickness was moderate, provided adequate fuel volume, and allowed the control-surface trailing-edge angles to be small enough to prevent high-speed buzz.

The choice of wing aspect ratio was based on studies of the variation with aspect ratio of weight empty, cruise fuel, second-segment-takeoff limiting weight, and operating cost. Payload, range, and field-length requirements were held constant. On a twin-engine transport airplane, single-engine climb performance in the takeoff and enroute configurations often limits the maximum usable weight. Since increased aspect ratio lowers induced drag and increases the critical climb performance, twin-engine airplanes tend to have higher aspect ratios than four-engine airplanes. Higher aspect ratio raises the gross weight required to perform a mission, because

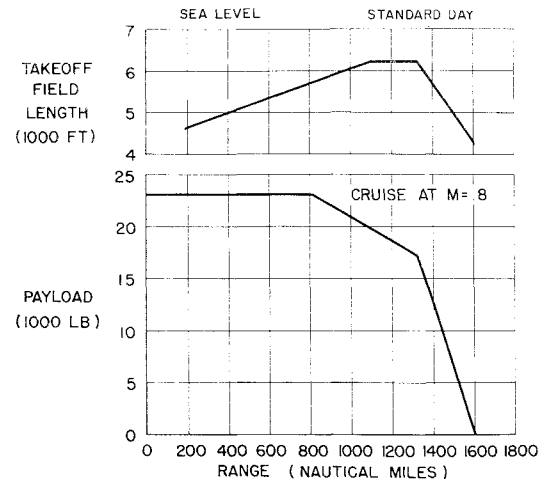

Fig. 2 DC-9 Series 10 performance summary.

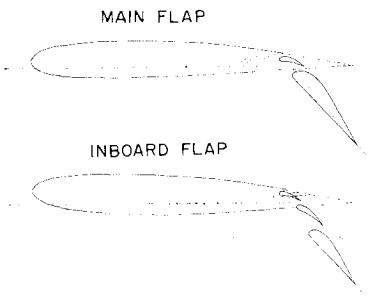

Fig. 3 DC-9 Series 10 high-lift system.

of the higher weight empty resulting from higher aspect ratio. For a short-range airplane, the weight-empty increase is relatively larger than the gain in fuel due to the lower induced drag. Nevertheless, the ability to carry greater weight from a given airport more than offsets the weight-empty increase until the aspect ratio reaches 8.0 to 9.0. The aspect ratio of the DC-9 Series 10 was selected as 8.25. The wing thickness distribution and the variation of airfoil shape across the span were chosen to give a constant drag-divergence Mach number from the root to the tip of the wing.

It was fortunate that the DC-8 development had produced a set of airfoils that had excellent high-speed drag characteristics as well as exceptional high-lift characteristics. Since the DC-9 Series 10 had severe short-field-length requirements and was not to have leading-edge devices, the use of these especially effective high-lift airfoils was essential. At the root and tip the airfoils are modified to correct for the finite-wing effects, that is, the changes in pressure distribution from leading edge to trailing edge induced by either the root or the tip effects of the swept wing.

Engine Location

The next major design decision was that of engine location. The choice of fuselage-mounted engines over wing-mounted engines was carefully considered. One of the important arguments for the aft location is the higher maximum lift coefficient that comes from a clean wing leading edge and from a flap uninterrupted by an opening for jet exhaust or for nacelles. Another important advantage is the reduction of cruise drag that comes from eliminating wing-pylon interference. Of course, there can be just as much interference between the nacelles and the fuselage with an aft-engine location, unless great care is taken in the aerodynamic design of the pylon, the nacelle, and the fuselage in this area. A third advantage is the reduction in the asymmetric-thrust yawing moment that exists when one engine is out. Another significant gain is the reduction in pylon-wing interference drag at the higher lift coefficients of the takeoff-climb condition. Since performance in the second-segment takeoff climb is especially important on a two-engine airplane, the beneficial effect of eliminating the pylon on the wing was probably the dominant performance factor in the decision to mount the engines aft.

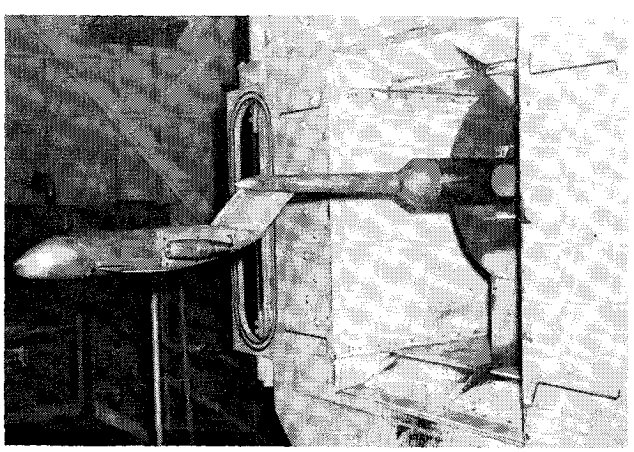

Fig. 4 Model used for investigation of nacelle configuration.

There are many nonaerodynamic factors that also must be considered, and their net effect cannot be determined without a detailed numerical analysis of a particular configuration. Our studies showed that the net effects of the aft-engine location on drag and weight were relatively small, except in the second-segment climb condition, where a worthwhile drag reduction was obtained.

Tail Configuration

The basic tail arrangement was the result of extensive study. The most efficient from the standpoint of weight and drag was the high horizontal-tail position. In this position, the horizontal tail endplates the vertical tail and reduces the required size of the vertical tail. The high sweep of the vertical tail results in a greater horizontal-tail length; that is, the position of the horizontal tail can be farther aft when the horizontal tail is placed on top of the vertical. Furthermore, the high tail is in a region of reduced downwash from the wing. These two factors reduce the size of the horizontal tail necessary for both control and stability requirements. The question of the optimum height of the horizontal tail arose again during the consideration of deep-stall control. At that time, wind-tunnel studies showed that for the DC-9 wing-fuselage-nacelle geometry tail height was not a significant factor.

High-Lift System

Since the DC-9 Series 10 design emphasized simplicity and maintainability, leading-edge devices were not used. The trailing-edge flap (Fig. 3) is a powerful, 36% chord, double-slotted flap, which rotates about a fixed external hinge. The position of the vane with respect to the flap is fixed. The flap span extends to 67% of the wing span. The inboard portion of the flap, which had to be modified because of structural clearance requirements, is a 3-slot flap with two vanes, which nest together with the flap in the retracted position.

Control-System Configurations

The primary considerations for selection of the flight-control systems were the use of proven concepts and proven, reliable hardware, to minimize development and maintenance problems. The DC-9 primary flight controls consist of conventional ailerons, rudder, and elevators. Lateral control also is provided by the flight spoilers, located ahead of the flaps on the wing upper surface. The spoilers also are used as speedbrakes for deceleration in the air and to decrease lift and increase drag during the landing ground roll.

Longitudinal control is provided by conventional aerodynamically balanced elevators with aerodynamic boost link tabs. Longitudinal trim capability is provided by the adjustable-incidence, electrically driven horizontal stabilizer. Pilot forces are derived from aerodynamic hinge moments and a two-rate control-column centering spring. A Mach trim compensator is provided in the longitudinal control system to assure a stable force variation with speed throughout the flight envelope.

A combination aileron and spoiler lateral-control system is used. The single aileron on each wing is balanced aerodynamically and boosted aerodynamically by a control tab. The wing spoiler system consists of three hydraulically powered spoilers in each wing: the inboard spoilers, i.e., the ground spoilers, operate only on the ground; the center and outboard spoilers, i.e., the flight spoilers, operate as speedbrakes in the air, as ground spoilers on the ground, and as the lateral-control spoilers at all times. The lateral-control function of the

flight spoilers provides up to 60° spoiler angle with the speedbrakes up or down, depending on the blowback characteristics. Because of intentionally limited hinge-moment capability, spoiler blowback to angles less than 60° will occur at airspeeds above approximately 180 knots. Lateral trim capability is provided by cable-operated trim tabs on each aileron. Aileron wheel forces are derived from both aerodynamic tab hinge moments and from load-feel springs located at each aileron.

Although the aft-fuselage engine location greatly reduces yawing moment caused by asymmetric thrust, a powerful rudder still is required to obtain good crosswind capability and low minimum control speeds. The rudder is aerodynamically balanced and hydraulically powered. Reversion to conventional aerodynamic tab control is automatic in case of loss of hydraulic-system pressure.

Rudder-pedal forces are supplied by load-feel springs for power operation and by the springs plus aerodynamic hinge moments with power off. The rudder trim system utilizes the load feel springs for both power-on and power-off trim. Directional control on the ground is improved by incorporation of rudder-pedal nosewheel steering. A series yaw damper without feedback through the rudder pedals is included in the directional-control system to improve dynamic stability characteristics for normal operation.

3. Aerodynamic Development

Wind-Tunnel Programs

A large part of the aerodynamic design development of the DC-9 was accomplished through the use of five major wind-tunnel models. Two of these were used in the solution of particularly unusual problems. They were a high Reynolds number aft-fuselage model with a simulated wing and nacelles and pylons for detailed drag optimization studies on the nacelle, pylon, and fuselage area, and a high Reynolds number low-speed model to obtain maximum-lift and stall-characteristics data.

Nacelle Design—Drag

One of the areas of the DC-9 design which differed fundamentally from previous Douglas designs was the aft-engine location. Placing the engines at the sides of the aft fuselage introduced the possibility of a drag problem because of boundary-layer separation in the divergent portion of the convergent-divergent channel formed by the nacelle, the pylon supporting the nacelle, and the adjacent part of the fuselage. In addition to low drag, the objectives in the design of the nacelle installation were light weight and simplicity.

A special wind-tunnel model was used to determine the optimum nacelle-pylon configuration. The two main considerations dictating the use of a nonstandard model were 1) the need to simulate, at wind-tunnel Reynolds number, the same fuselage boundary-layer thickness (nondimensional) at the nacelle which would exist on the airplane in flight; and 2) the need to eliminate the conventional fuselage sting support that would, unrealistically, relieve the flow divergence over the aft portion of the fuselage. The resulting model, consisting of a foreshortened fuselage and dummy wing, was supported by a sting attached to the top of the vertical tail (Fig. 4).

The variables evaluated during the wind-tunnel-test program included the gap between nacelle and fuselage, pylon thickness and planform, nose-cowl length and camber, afterbody and terminal-fairing designs, and many others that pertained to detail design problems. Probably the most important part of the program was the investigation of the effects of nose-cowl length and camber. The camber was important because it was desirable to have a symmetrical

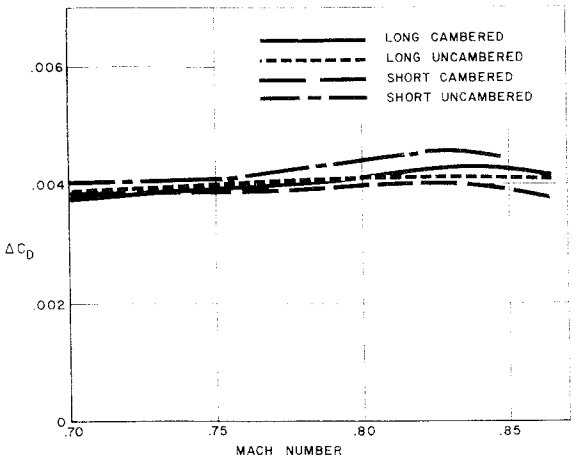

Fig. 5 Effect of nose-cowl length and camber on nacelle-pylon incremental drag.

(uncambered) nose cowl, so that the left and right nose cowls would be interchangeable. Some of the results of this investigation are presented in Fig. 5, where the drag increment caused by the nacelle and pylon is shown as a function of Mach number for four of the configurations tested. Note the significant drag rise of the short, uncambered configuration, beginning at a Mach number below 0.8, as opposed to the drag rise of the short, cambered configuration, which remained very slight to a Mach number well beyond 0.8, the highest cruise Mach number of the DC-9. Although the drag rise of the uncambered configuration could have been greatly reduced by lengthening the cowling, the added weight and friction drag (internal and external) relative to the short, cambered configuration ruled that out in spite of the interchangeability advantage. The effect of the cambering was to minimize the acceleration of the flow in the channel between the fuselage, pylon, and nacelle.

Nacelle Design-Wake Ingestion

Another problem area associated with engines mounted on the aft fuselage was the possibility of engine operating difficulties because of ingestion by the engines of wakes from various components of the airplane. Extensive wind-tunnel tests were conducted at low and high speed in order to determine the total-pressure distortion patterns that appear at the engine compressor face when wakes are drawn into the inlet. The variables that were investigated included ground effect, inlet mass-flow ratio (engine power setting), flap deflection, spoiler deflections, angle of attack, yaw angle, and Mach number.

The inlet survey tests showed that the fuselage wake does not enter the inlet at sideslip conditions, and that the total-pressure distortions created by the ingestion of the spoiler wake or the wing wake do not exceed the allowable 5% limit at either low or high Mach numbers, except at conditions well beyond the buffet boundary. It later was found from flight tests that, at and beyond the stall with power on, there is considerable engine surging or popping. This, however, does not only not interfere with engine operation but actually is considered a favorable factor in that it provides an additional, unmistakable stall warning.

Stall and Deep Stall

Satisfactory stall characteristics have always been an important design criterion for any airplane. Requirements for adequate stall warning, for strong natural pitchdown at the stall for inherent recovery, and for good lateral control through the stall were established during the conceptual stages of the DC-9. Transport-airplane characteristics at angles of attack

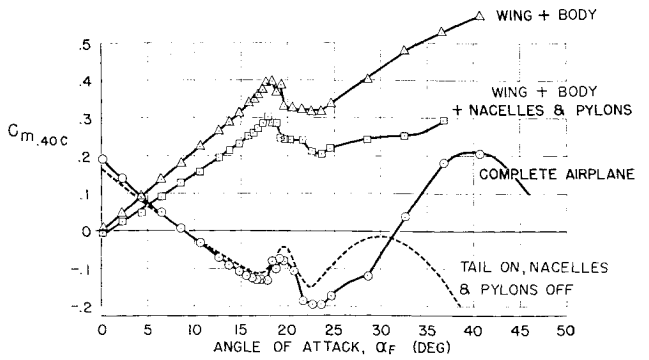

Fig. 6 Pitching-moment buildup, flaps up. Typical model with deep-stall problems.

far beyond the stall have not usually been given very much consideration, for several reasons. First, transports are almost never stalled except in test programs; second, stall is so clearly indicated that rational pilots recover from the stall before the angle of attack increases much beyond the stall angle; and, third, there has never been any reason to explore the region of very high angle of attack. It has been known for some time that pitching-moment curves of certain T-tailed designs tend to show an unstable region at angles well beyond the stall. This instability was brought into sharp focus by the unfortunate accident of the BAC-111. Fear of the high-angle-of-attack stall became widespread, and studies of extreme angles of attack were initiated all over the world.

Before discussing the physics of the deep stall, we first must define the term. The normal stall region can be defined as the angle-of-attack range starting with the angle for maximum lift and extending for from 4° to 6° beyond it. Very few flight explorations of the angle-of-attack range beyond this have been carried out in the past. Since airplanes normally stall at angles from 15° to 20°, angles of attack beyond 25° have not usually been experienced. The deep stall may be defined as a stall at an angle of attack above 25°, but, in truth, the deep stall with which we are concerned occurs in the region from about 35° to 50° angle of attack. Now, if we call this the deep stall, we must further define the term locked-in deep stall. This represents a stable condition at an angle of attack of 40° to 50°, from which no recovery is possible. An intermediate case might be a condition in which, with certain settings of controls, the airplane can assume a stable trimmed attitude at an angle of attack in the deep-stall region and therefore have a stable deep stall but still be recoverable through motions of the controls. This would not be a locked-in deep stall.

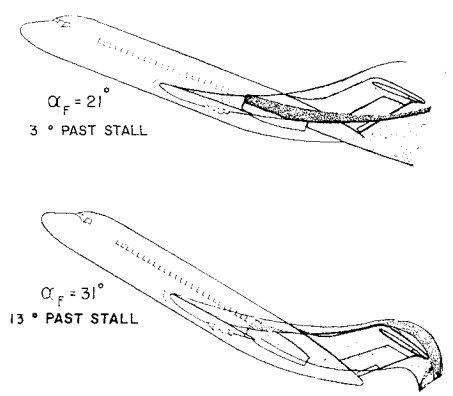

Fig. 7 Wake location beyond stall, flaps up, low Reynolds number.

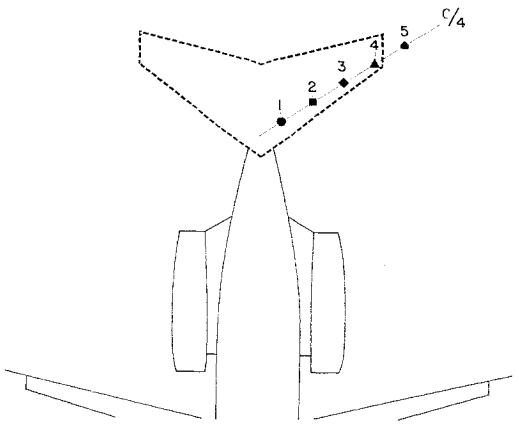

Fig. 8 Wind-tunnel-model probe locations.

The Stall Problem

The first phase of the DC-9 deep-stall study was a basic experimental investigation of the aerodynamics of the deep stall. Figure 6 shows wind-tunnel pitching-moment coefficients of an aft-engine T-tail configuration that has a stable and locked-in deep stall. Curves are shown for 1) the wing and body alone, 2) complete airplane, 3) airplane without tail, and 4) airplane without nacelles and pylons. Notice that the tail-off model is mildly unstable, as is to be expected for any design, and shows a stable nose-down moment break at the stall. At angles far beyond the stall, no unusual behavior is seen. Adding the nacelle to this configuration increases the stability slightly, since the nacelle and pylons act as a tail of low aspect ratio and short tail length. Adding the tail to the configuration produces a curve that has a small unstable break at the stall, followed by a narrow pitch-down region, followed at angle of attack beyond about 21° or 22° by a strong unstable characteristic. The pitching moment becomes less and less negative and finally, at angles of about 32° and beyond, becomes positive, or nose-up. Above about 42° the curve bends, again becoming stable. At these angles of attack, the elevator effectiveness is very low, so that application of full nose-down moment is not adequate to produce a negative pitching moment. The airplane then is stable and locked into a deep stall. Pitching moments without the nacelle were similar up to about 28° but then became stable and did not indicate a locked-in deep stall. It was clear that the nacelle contributed substantially to the problem.

The next phase of the investigation analyzed the flow induced by each airplane component contributing to these pitching-moment curves. Visual investigations of the wing and nacelle wake patterns were carried out by means of streamers from the leading and trailing edges of the wing and the nacelle-pylon. Figure 7, an example of this type of observation, shows that the tail remains in the wing wake to a much higher angle of attack than it does with low-tail arrangements. Furthermore, when the tail begins to move out

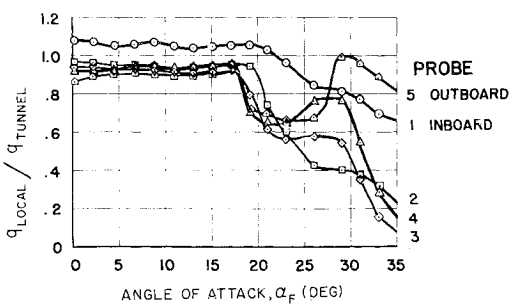

Fig. 9 Dynamic pressure ratio at the tail, flaps up.

of the wing wake, it runs into the nacelle wake, so that the dynamic pressure over the tail is adversely affected through a very large angle-of-attack range.

A complete survey of the angle of attack and dynamic pressure at the tail was obtained for airplane angles of attack up to 35°. Figure 8 shows the location of the probes across the span of the tail. The dynamic pressures are shown in Figure 9. It can be seen that the dynamic pressure at the tail is close to that of the freestream and quite uniform across the span up to the angle of stall; above this angle the dynamic pressure starts to decrease. The decrease rapidly becomes very large, and at angles of attack around 35° the loss in dynamic pressure becomes as high as 80% of the freestream value across most of the tail span. It is notable, however, that as the angle of attack increases beyond 26°, the dynamic pressure of the most outboard station tested begins to increase rapidly.

Figure 10 shows the tail angle of attack from the same survey. The angle of attack of the horizontal tail is uniform and shows just about the predicted downwash up to the stall. Shortly beyond the stall, the inboard section of the tail shows tremendous downwash, whereas the outboard section shows very large upwash. Figure 9, the variation of dynamic pressure, shows that the decrease in dynamic pressure was much less over the inner portion than over the outer portion of the tail, so that the part of the tail with high dynamic pressure is the part with the down load due to the high downwash. This contributes strongly to the pitch-up tendency.

Such an extreme downwash pattern is indicative of a vortex. An exploration with probes and smoke pictures proved that this downwash pattern was indeed a result of lifting vortices shed from the fuselage. Various attempts to change the characteristics of this vortex pattern were not successful.

Figure 11 shows the results of investigations of control effectiveness. The variation of pitching-moment coefficient with stabilizer incidence $C_{M_{i_H}}$ and the variation of pitching moment with elevator angle $C_{M_{\delta_e}}$ both show a large decrease in effectiveness at the higher angles of attack. The deep-stall instability thus is shown to be caused by a combination of wing and nacelle-pylon wakes that degrade the tail-surface effectiveness, with an additional adverse contribution from fuselage vortices.

Developing the DC-9 Stall-Characteristics Requirements

Once an understanding of the basic characteristics of the stall and deep-stall phenomena had been developed, a philosophy for the design of the DC-9 was established. First, the problem was divided into two parts: the normal stall, up to perhaps 5° or 6° beyond the stall, and the deep-stall region, at angles of attack up to about 50°. For the normal stall, the philosophy was the same as that used for any Douglas transport airplane. Specifically, there must be strong natural or artificial stall warning. At the stall, there must be a strong natural pitchdown to mark the stall; lateral-control effectiveness must be retained through the complete stall region; and control response must be effective immediately when recovery from the stall is initiated by the pilot. It also was desired that pilot cues indicating the presence of the stall become increasingly obvious as the stall is entered. For the deep-stall region, the requirement was established that normal recovery capability be available from any angle of attack, even though it would be almost impossible for a rational pilot to go beyond the normal stall region.

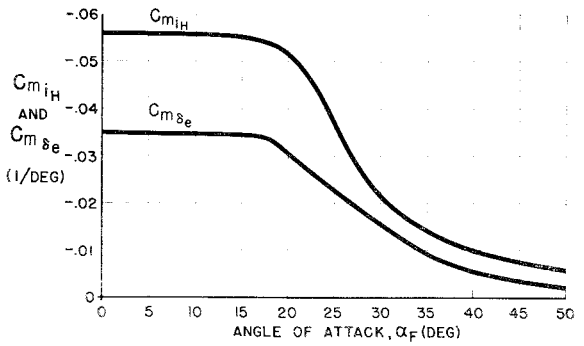

Fig. 11 Stabilizer and elevator effectiveness.

The wing was designed to stall first at about 35% semispan, leaving the outer panel and the root unstalled for about 2° beyond the initial stall angle of attack. It was originally thought important to avoid stalling the root, for fear of wake ingestion by the engine. The maximum lift coefficient across the wing was controlled by varying the shape of the leading edge, since the basic airfoil contours were based on high Mach number requirements. Early wind-tunnel tests showed that this philosophy was not adequate, although the same procedure had worked very well on the DC-8. Spanwise flow on the wing caused stall too early on the outer panel, resulting in some minor pitchup at the stall. Furthermore, the pitchdown moment available in the deep-stall region was not adequate to assure positive pitchdown capability to the pilot at the critical aft center-of-gravity position. A very extensive wind-tunnel program was undertaken, which involved the variation of airfoils across the span, many types of fences on upper and lower wing surfaces, leading-edge-stall strips, various vortex-generator configurations, and tail-size and tail-location variations. Various devices on the aft fuselage and nacelle were tested to create more nose-down pitching moment at the very high angles of attack. Analysis of many configurations tested in the wind tunnel led to a simple and most satisfactory configuration.

The solution of the normal stall problem was an underwing fence and an increase of about 20% in the span of the horizontal tail (Fig. 12). In the deep-stall regime, the larger

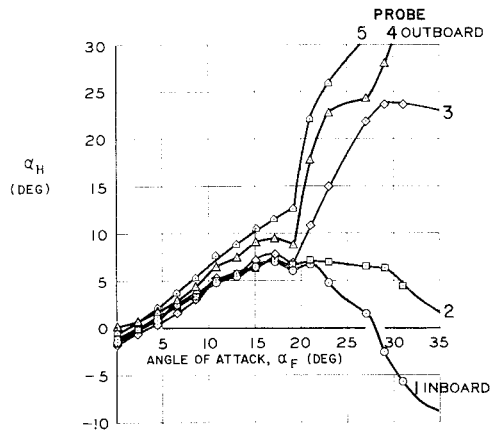

Fig. 10 Angle of attack at the tail, flaps up.

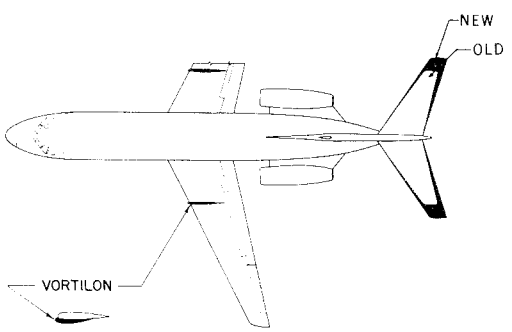

Fig. 12 DC-9 modified horizontal tail and vortilon.

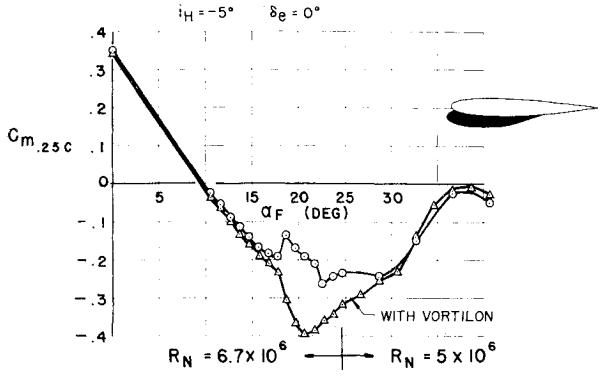

Fig. 13 Effect of vortilon on pitching moments, flaps up, high Reynolds number.

horizontal tail and an auxiliary power-augmentation system on the elevator solved the problem.

It is well known that leading-edge fences have been used to improve pitchdown characteristics at the normal stall. However, a leading-edge fence also creates vortex drag at angles of attack important to the second-segment climb, and has some cruise drag penalty because of the disturbing effect on the wing aerodynamic sweepback. A special type of underwing fence therefore was developed, which we called a vortilon (vortex-generating pylon). This underwing device does not create a vortex, except at angles of attack beyond those of any interest to performance. For cruise and takeoff climb conditions, the wing stagnation point is ahead of the leading edge of the vortilon. As the stall is approached, the stagnation point moves aft of the intersection of the leading edge of the vortilon with the wing, and the interference with the leading-edge crossflow creates a strong vortex that goes over the top of the wing. This vortex has two basic effects. First, it scours the boundary layer flowing from the inner to the outer part of the wing upper surface and reduces the detrimental effect on the outer-panel maximum lift. Furthermore, the vortex creates an upwash field inboard of the vortilon. This upwash acts on the tail to create a pitchdown at the stall that continues to more than 10° beyond the stall. Figure 13 shows a pitching-moment curve with and without the vortilon. The vortilon changes an unstable break at the stall to a sharply stable one. Figure 14, the pitching-moment contribution of the vortilon, tail-on and tail-off, shows that more than half of the effect is from the tail contribution. Results of testing the vortilon in several spanwise positions showed the 35% semispan location to be most effective.

The vortilon was very effective with flaps up and at low flap angles, but at full flap deflection (50°) it was relatively ineffective. Fortunately, the horizontal-tail extension solved the problem. But it, too, was not effective alone; at full flap deflection, it took both vortilon and horizontal tail to provide positive pitchdown.

The larger span tail also provided pitchdown capability at any angle of attack up through and beyond the deep stall.

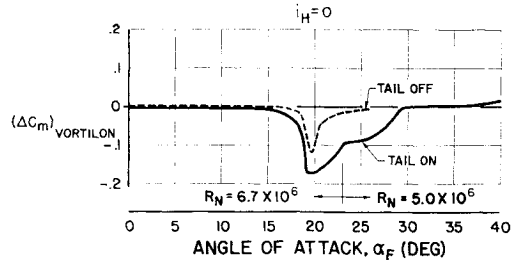

Fig. 14 Contribution of vortilon to pitching moments, flaps up.

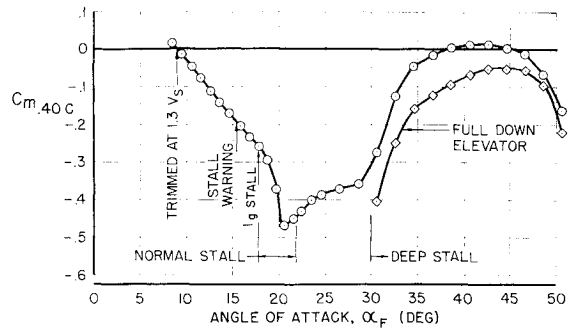

Fig. 15 Pitching-moment coefficients for DC-9 Series 10 configuration, flaps up.

The extended tip, with the improved dynamic pressure environment, is in a region where there is considerable upwash induced by the fuselage vortices. The horizontal tail produces the desired negative moment at the most aft center-of-gravity position at any angle of attack, provided the elevator reaches the full-down position. This led to the second configuration change to meet our deep-stall design requirements, namely, a power-augmentation system for the elevator.

At angles of attack beyond about 30°, the effectiveness of the aerodynamic-boost linked tab that drives the elevator decreases rapidly. For this condition, a hydraulic power augmentation system was developed to provide full-down elevator control under extreme adverse angle-of-attack conditions. This system applies trailing-edge-down elevator hinge moment whenever the control tab exceeds an angle of 10° trailing edge up. The highest tab angle normally used is 8°. The system does not operate in the elevator trailing-edge-up direction. The angle to which the elevator is driven by the power system is determined by how far the pilot pushes the wheel forward. The hinge-moment capability of the system is moderate, since it is required only at the low dynamic pressures associated with deep stall. The power system actuates only if both left-hand and right-hand elevator control tabs exceed 10° deflection, to insure fail-safe operation.

The wind-tunnel wake studies indicated that aerodynamic stall warning before the actual stall probably would be light; therefore, two completely redundant stall-warning systems were provided. Two tab-type leading-edge angle-of-attack sensors are combined with completely independent electrical and stick-shaker systems.

The final wind-tunnel pitching-moment characteristics obtained at a Reynolds number of approximately 7 million are shown in Figs. 15 and 16 for 0° and 50° flaps, respectively, for the most aft center-of-gravity position. The stick-shaker stall warning occurs well before the stall. At the stall, a strong pitchdown occurs, followed at a considerably

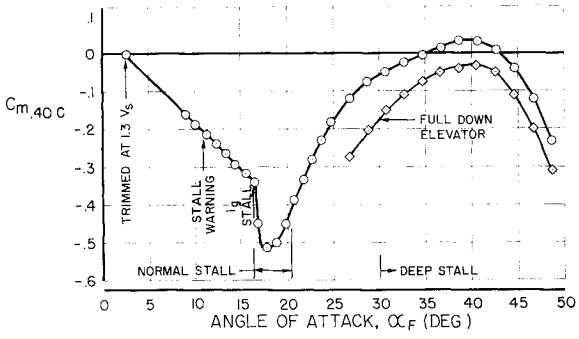

Fig. 16 Pitching-moment coefficients for DC-9 Series 10 configuration, flaps 50°.

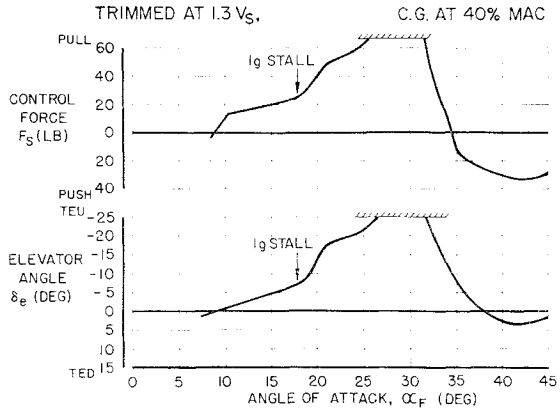

Fig. 17 Control force and elevator angle required to balance pitching moments, flaps up.

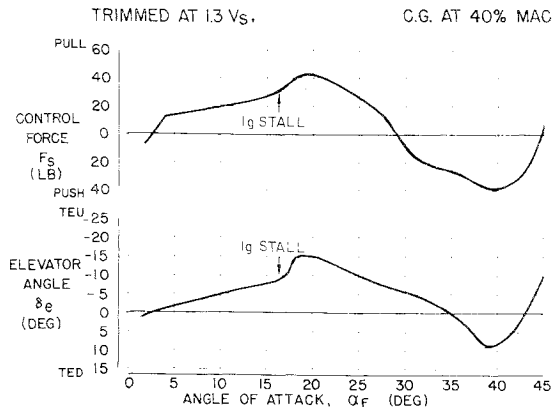

Fig. 18 Control force and elevator angle required to balance pitching moments, flaps 50°.

higher angle of attack by a reduction in pitchdown moment. The pitching moment then becomes less and less negative, but requires 7° to 10° of angle-of-attack increase above the stall before the pitching moment is less negative than it was at the stall. Eventually, at very high angles, the pitching moment becomes slightly positive with zero elevator angle; but, with full down elevator, the pitching moment will always become negative. It is significant that, as the center of gravity moves forward, the obtainable negative moment rapidly becomes very large, until at mid center-of-gravity positions it is not possible to get these extreme angles of attack even with full up elevator.

In order to interpret the pitching-moment characteristics in terms of the flying qualities, the control force and elevator angle to trim to zero moment were computed as functions of angle of attack. The results are shown in Figs. 17 and 18 for 0° and 50° flaps, respectively, again for the most aft center-of-gravity position. For 0°, the data show that it is not possible to reach a deep-stall attitude without exceeding the maximum up elevator angle of 25°. For a stall entered at a very high rate, the data indicate the possibility of dynamically coasting to the deep-stall region with this configuration. When nose-down elevator is applied, however, pitch-down moment always is obtained. With 50° flaps, it is possible with large up-elevator angles to reach excessive angles of attack, but only after passing artificial stall warning and overpowering a strong pitchdown, which requires considerable up-elevator deflections with corresponding pilot-force increases. Furthermore, the wind-tunnel model indicated powerful aerodynamic buffeting at angle of attack beyond the stall, to further reduce the likelihood of an inadvertent deep stall. It was concluded that these represented excellent characteristics.

Analog Computer and Simulator Studies

In order to evaluate the data obtained from the wind tunnel in terms of dynamic maneuvers, extensive analog-computer studies were conducted. Later in the program, the analog computer was connected with a simulated cockpit to create a very effective simulator. Many of the possible pitchdown characteristics at the stall and the pitching-moment characteristics through the deep stall were evaluated by our flight personnel in order to determine the optimum configuration. On the basis of these results, our flight personnel expected the DC-9 to have excellent longitudinal stall characteristics.

4. Flight Development

Aerodynamic design development was continued during the first part of the flight-test and certification program. The primary aerodynamic characteristics requiring continued development were roll characteristics at the stall and lateral-control-system response. Improvements in takeoff-climb performance also were achieved.

Stall Characteristics

Flight-test stalls were characterized essentially by no aerodynamic buffet prior to the operation of the artificial stick shaker, a well-defined g break at the 1-g stall, a good airplane nose-down pitching at the g break, and, on the majority of the stalls, a strong random roll at or immediately following the 1-g break. This rolling motion, when it occurred, was so rapid that bank angles up to 30° could be generated easily before lateral-control action by the pilot could stop the bank-angle buildup. The 1-g stall speeds obtained during these flight tests were somewhat lower than those used in the performance predictions.

Flight tests with wing tufts indicated that stalling occurred first at the leading edge at about midspan and spread rapidly inboard and outboard. When this occurred asymmetrically, a strong, rolling acceleration developed. The rolling acceleration was accentuated by the relatively large lift loss typical of high-lift airfoils at the stall, and by the low moment of inertia in roll of the aft-engine configuration. An intensive flight program was carried out to develop a configuration that would achieve the excellent stall character-

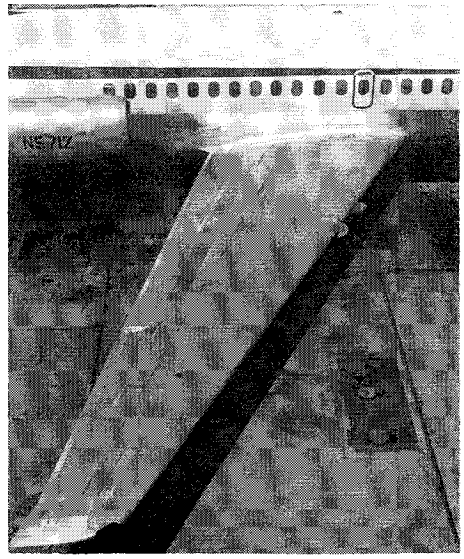

Fig. 19 Wing modifications: stall strips and leading-edge fence.

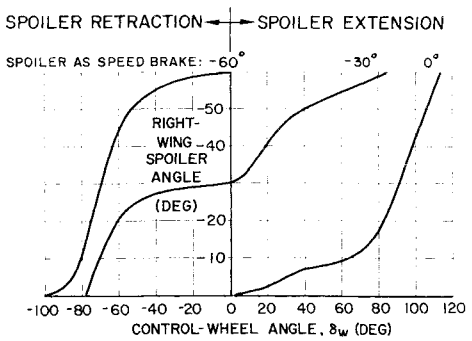

Fig. 20 DC-9 flight-spoiler characteristics.

istics considered essential for the DC-9, and at the same time obtain the low stall speeds required for takeoff and landing performance. This program developed two minor but effective modifications in wing geometry, shown in Fig. 19. The first modification is an inboard stall strip, approximately 42 in. long, located on the wing leading edge at the wing root. This device assures initial wing stalling at the wing root. Next, a small leading-edge fence was added at approximately midspan. The primary action of this fence was to confine the initial stall to the inboard area of the wing, so that right and left wings would stall inboard before the stall progressed toward the tip. Originally, two rows of vortex generators were added on the outer wing panel from approximately 60 to 85% semispan, in order to reduce the severity of the outer-panel stall. These were removed when the other changes made the generators unnecessary.

These wing modifications resulted in stalling characteristics that pilots describe as outstanding, while providing a level of stall speeds compatible with the short-field-performance requirements. During the stall program, over 1800 stalls were made at all flap configurations, engine power on and off, straight and turning flight, and with wing spoilers up and down. These tests have been carried out up to angles of attack of 28° at full aft center of gravity at approach rates in excess of 4 knots/sec. Final stall characteristics include very light aerodynamic buffet occurring after the dual stick-shaker warning, strong inherent nose-down pitching beyond the g break, very little rolling tendency, and moderate to heavy buffet after the stall, in conjunction with pronounced engine popping or banging at all practical inflight power settings. By virtue of its strong inherent recovery characteristics and the existence of unmistakable pilot warning cues that stall has been reached, the DC-9 is extremely resistant to entering the deep-stall region. Pitching characteristics during the stall in flight and in the simulator were found to be in excellent qualitative agreement.

Lateral-Control System

Another area of flight development related to aerodynamics was the lateral-control system. Early flight tests

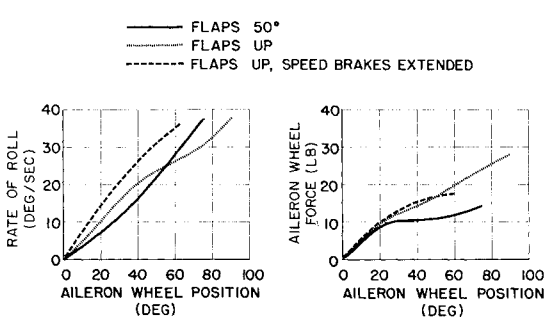

Fig. 21 DC-9 lateral-control characteristics.

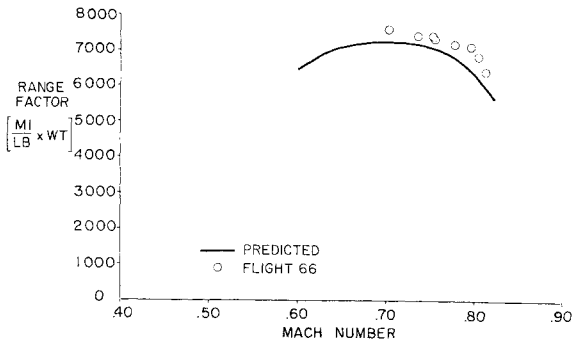

Fig. 22 DC-9 flight-test range performance; W/δ = 30,000 lb.

confirmed the powerful lateral-control capability associated with the spoiler-aileron lateral-control system, especially in the landing configuration. However, flight-test data obtained during landing approaches in gusty conditions showed that pilots had a tendency to over-control and had some difficulty in maintaining bank angle within desirably tight limits. Further flight tests indicated that lateral-control-system spring-force characteristics, friction level, and spoiler-aileron mixing were the prime contributors to this over-control tendency. Intensive design effort has produced a system with pleasantly light forces, extremely low friction, and nearly optimum response, not only in the landing-approach configuration, but also in the takeoff, climb, cruise, and descent conditions. The characteristics of this lateral-control system are shown in Figs. 20 and 21.

Performance

The stall-characteristics fixes had some adverse effect on takeoff-climb drag, an extremely important factor in determining payload capability from high-altitude airports or from airports where hot day conditions prevail. It was found that reserve wing strength built into the DC-9 Series 10 would permit the addition of a 1-ft wing-tip extension on each side. This improvement essentially counteracted the drag of the stall strip and fence.

Although an aerodynamic flight-development program was required for the three examples discussed, most of the aerodynamic characteristics required no flight research. Particular examples are cruise performance, aerodynamic flight-control systems, and engine-inlet nacelle and pylon configurations. For example, Fig. 22 shows a comparison of estimated range constants with flight-test range constants at a weight-to-pressure ratio W/δ = 300,000, corresponding to long-range-cruise operation at 30,000 to 35,000 ft. This comparison shows that cruise performance compares favorably with predictions.

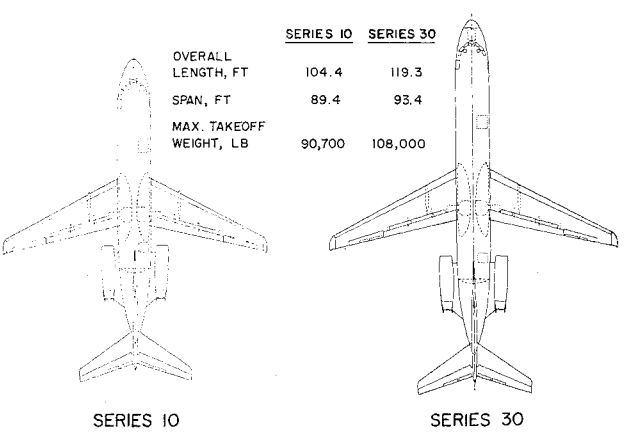

Fig. 23 DC-9 configuration comparison.

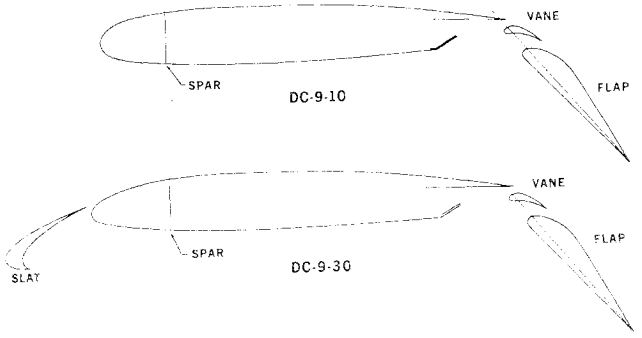

Fig. 24 High-lift systems.

5. Future Development

Almost all airplanes have follow-on versions, but very few have them under construction before the original airplane enters service. The DC-9 Series 30 has a fuselage longer than that of the series 10 by 179 in., wing span greater by 4 ft, a wing-chord increase of 6%, and leading-edge slats. Figure 23 shows a comparison of the external dimensions of the two airplanes, and Fig. 24 illustrates the difference in the high-lift systems.

Since the Series 30 is equipped with leading-edge slats, and the maximum lift coefficient is much less dependent on the shape of the airfoil leading edge when slats are used, the airfoil ahead of the front spar is entirely different on the Series 30 airplane. The chord is extended by 6% and the contour redesigned to minimize the gradual drag rise before the drag-divergence Mach number, at the expense of basic-airfoil maximum lift coefficient. With slats extended, the maximum lift coefficient is very little different from what it would have been if the original airfoil had been retained. The result is an improvement in specific range in the cruise region and a very large increase in the maximum lift coefficient in the takeoff and landing regimes with slats extended. Use of slats required extensive wind-tunnel optimization of slat angle and position to optimize maximum lift coefficient, slat drag in ground acceleration, and slat drag in the takeoff-climb configuration.

The flight-control systems of the Series 30 are essentially identical to those of the Series 10. The roll problem experienced at the stall with the Series 10 is not expected to occur with the Series 30, since by the nature of the slat design and the variation of slat effectiveness across the span, there is very little loss of lift until several degrees beyond the stall angle. Therefore there is essentially no rolling moment at the stall. No need for such devices as the leading-edge fence or the stall strip is anticipated.